УДК 517.9:621.325.5:621.382.049.77
M. KOSOVETS,
SPE «Quantor», Kyiv;
L. TOVSTENKO,
Institute of Cybernetic of Gluchkov National Academy Scientific of Ukraine, Kyiv

Modeling conical horn antenna of 3D terahertz FMCW radar

The possibility of forming aperture of conical antennas is studied, as well as measuring of near and far-field antenna is realized. Research the effect of the absorber on the size of the antenna pattern in the frontal area.

Keywords: digital spectral analysis; horn of antenna; electromagnetic simulators; Maxwell's equation; method of moments; finite elements method; finite differences in the time domain; finite integration technique.

INTRODUCTION

In scientific laboratories SPE «Quantor» designed and manufactured **FMCW** (*Frequency Modulation Continuous Wave*) radar with the following parameters: frequency band linear frequency modulation — from 92 to 96 GHz; period (length of interval) — 1 ms; bit ADC — from 16 to 32 bits; the number of cycles of accumulation — from 1 to 10000; reflection layers — 3; distance to reflection layers — 0.095, 0.105, 0.106 m; wave propagation environment — air; signal-to-noise ratio — from 80 to 30 dB.

We used conical horn antenna. According to the theory of equivalence constructing antennas extend to higher frequencies in the terahertz range.

To study the main characteristics of the various methods of spectral estimation parameters of signals were field tested in order to create a test model determinate harmonic signal.

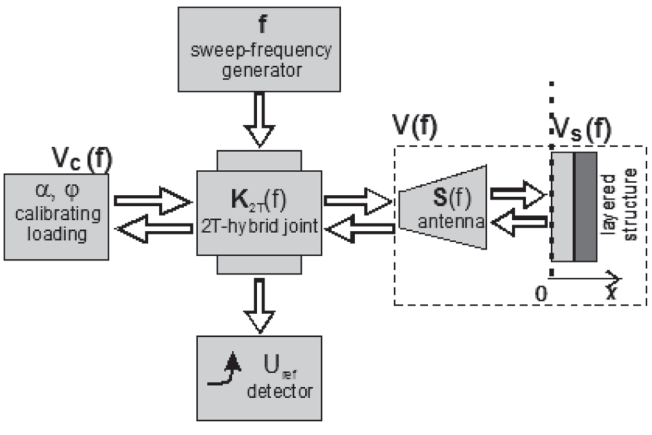

The reflection coefficient of antenna-layered structure:

$$V(S_1,S_2,S_3,V_S)=S_1+\frac{S_2V_S}{1-S_3V_S},$$

where S_1, S_2, S_3 are the coefficients of model;
V_S — the reflection coefficient of the medium;

$$S_1=S_{11}^{\mathrm{A}},\ S_2=S_{12}^{\mathrm{A}}\cdot S_{21}^{\mathrm{A}},\ S_3=S_{22}^{\mathrm{A}},$$

where $S^{\mathrm{A}}[2\times2]$ — the scattering matrices of the antenna.

The goal function:

$$F_3(S_1,S_2,S_3)=\sum_{i=0}^{Nx}\left|V_{\mathrm{et}}^{\mathrm{ex}}(x_i)-V\left(S_1,S_2,S_3,V_{\mathrm{set}}^{\mathrm{th}}(x_i)\right)\right|^2,$$

$$(S_1,S_2,S_3)^*=\inf_{|S_i|<1}F_3(S_1,S_2,S_3).$$

Here $\left|V_{\mathrm{set}}^{\mathrm{th}}\right|=1$, $\arg\left(V_{\mathrm{set}}^{\mathrm{th}}\right)=2\cdot2\pi x/\lambda_0$ — theoretical reflection coefficient of the medium; $V_{\mathrm{et}}^{\mathrm{ex}}$ — the experimentally measured reflection coefficient of the medium.

MAIN PART. Conical horn antenna simulation

Formulation of the problem

The selection of high-frequency components (antennas, filters, packages and more) is heavily dependent on computer-aided design (CAD). Electromagnetic (EM) simulators are useful tools for reducing time and cost design. In many cases a proper usage of a EM simulator permits to obtain the required parameters even at the first prototype realized.

However, EM simulation as a numerical process suffers from systematic and random errors. Thus the setting of the EM simulator such as a frequency range, mesh properties, bounding box dimension, usage of PEC walls etc. has to be done with the highest attention and the simulation results have to be always verified and carefully analyzed.

EM simulators have at least one Maxwell's Equation (ME) solver. Simulators can be categorized on the basis of their solution method: Integral Equations (IE) solved by Method of Moments (MoM), Finite Elements Method (FEM), Finite Differences in the Time Domain (FDTD) and Finite Integration Technique (FIT) [1].

Although all these methods are valid, it is important to understand limits and scopes of each solvers. Using a specific solver, well designed for a particular electromagnetic problem, can time of computation can be greatly reduced. So a carefully survey of the simulation scenario it's necessary to decide the best solver to use.

MoM solves ME in integral form; the electromagnetic problem is described in terms of unknown currents flowing on the object to be simulated. The coupling between fields and current is obtained through a Green's function which includes the electromagnetic influence of the complete infinite «background» environment. By this way the solution is

accurate in every point of the background environment. Through analytic expression is possible to obtain far-field radiation.

Boundary equations expressing the physical nature of the object to be described (conductivity on a conductor, permittivity in a dielectric part of the object), are enforced. This is either done at the boundaries of volumes or inside the entire volumes themselves. IE-MoM gives rise to a dense matrix equation, which can be solved using standard matrix algebra technology.

MoM solvers operate in frequency domain, so it's needed to simulate at each frequency of interest. Like others frequency domain solvers MoM is not well suited for broadband problem. A time domain solver instead doesn't need this «sweep» frequency instead and can simulate in a wider frequency range with better performance.

For large electric structure MoM needs to solve a very dense matrix, that needs a huge amount of memory. De facto this limits MoM solvers for very complex structure and is instead well suited for open regions problems.

Furthermore, inhomogeneous materials are another weakness of MoM solvers. The dielectrics' inhomogeneity of the environment has to be described by Volume Integral Equations, leading to a number of unknowns proportional to the size of the object's volume + environment. Even if, in these cases, the number of unknowns in these cases is still below the number of unknowns for differential equation techniques, the dense coupling matrix of the IE-MoM technique requires much higher computational resources and in practice prohibits its use.

For simulations which involve complex structure and/or inhomogeneous material differential solvers are more advisable. The most popular differential methods are the Finite Element Method (FEM) and the Finite-Difference Time Domain method (FDTD). Since the number of unknowns is proportional to the volume and the resolution considered, differential equation methods are particularly suitable for modeling small full three-dimensional electromagnetic problems which have complex geometrical details and problem with wide band of interest.

FEM subdivides space in elements, for example tetrahedral. Fields inside these elements are expressed in terms of a number of basic functions, for example polynomials. These expressions are inserted into the functional of the equations, and the variation of the functional is made zero. This yields a matrix eigenvalue equation whose solution yields the fields at edges of the elements. FEM normally is formulated in the frequency domain, i. e. for time-harmonic problems. This means that, as for IE-MoM, the solution has to be calculated for every frequency of interest.

FDTD method is based upon time relation between fields E and H. From ME is know that the time derivative of the H-field is dependent on the curl of the E-field, and the time derivative of the H-field is dependent on the curl of the E-field. FDTD can compute the E field and the H one at any time using previous stored values of the fields. Obviously, time coordinate and space domain are discretized. For discretization of space is used Yee cell which can be described like a cube; the electric field components form the edges of the cube, and the magnetic field components form the normals to the faces of the cube. So it's clear that the fields are dependent not only by the previous stored value but also from the values of adjacent Yee cells (fig. 1) [2].

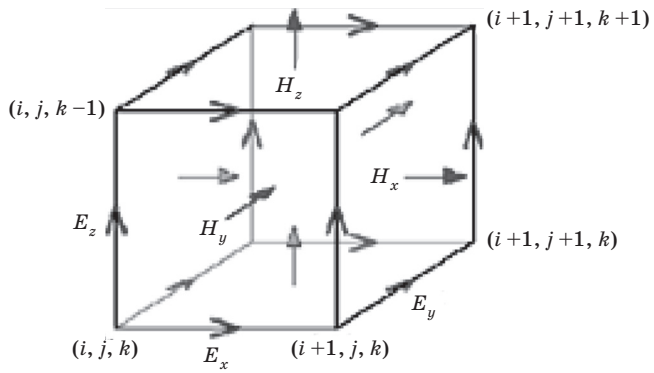

Fig. 1. Yee Cell in Cartesian grid: *i, j* and *k* are space indexes of the three-dimensional Yee lattice

The recursive method used for finding solution of ME can lead to instability so solvers need to provide an upper bound on the time-step to ensure numerical stability. Another solution is to stop simulation when EM energy in time domain fall below a certain threshold, in this case is obviously needed a pulsed excitation and not a periodic one.

For our simulation we use commercial tool CST MWS that use a modified version of FDTD called FIT (transient solver). This solver uses integral form of ME and it's the most important difference between FIT and FDTD. Transient solver is a good choice in our scenario due to high frequency of simulation and small dimensions of horn antenna.

Antenna design

Our horn antenna model has been designed using CAD tools provided in CST MWS. The geometrical parameters and their value in mm are summarized in the table 1 and shown in fig. 2.

Antenna is fed by a non-standard rectangular waveguide, 2.32×0.98 mm. The closer standard waveguide is the WR-8, 2.032×1.016 mm, designed to work in 90…140 GHz frequency band [3]. Due to the greater width we expect it works well in 92…96 GHz band, i. e. the frequency sweep of our microwave source.

Feed source has been designed with a waveguide-port using pick point feature to match edges of input waveguide. Horn antenna has been designed with flange and cylinder junction to obtain a more accurate simulation.

Table 1

Geometric parameters of antenna

Name	Value, mm	Description
L_1	28.2	Horn length
L_2	3.6	Cylinder length
L_3	3.2	Flange length
R_1	9	Extern radius of horn mouth
R_2	8	Internal radius of horn mouth
R_3	3	Cylinder radius
a	2.32	Waveguide width
b	0.98	Waveguide height
l	18	Flange side
h	1	Chamfer width

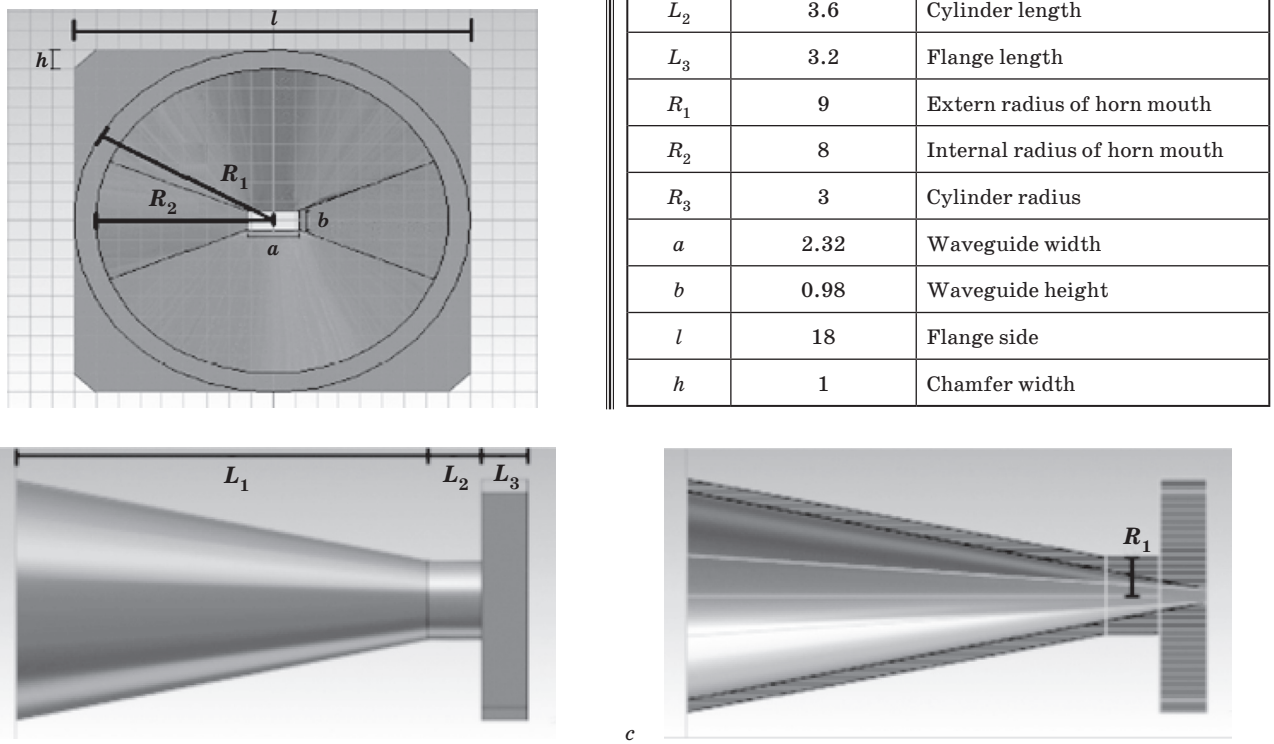

Fig. 2. Horn antenna:
***a* — front view; *b* — lateral view; *c* — Cut plane in YZ plane**

Near and far-field regions

We are interested both far-field and near-field patterns. Calculating the Fraunhofer distance we find that the transition zone is more or less at 2.5 m far from horn mouth.

A post-processing tool has been utilized to obtain near field patterns. We have computed patterns at some distances from horn mouth. The closer pattern is 1.25 cm far from horn mouth, which is the minimum distance possible to obtain through the tool. The farther pattern is 28.25 cm far from horn mouth, maximum distance of our interest.

Far-field result

Antenna is well matched in the frequency of our interest. In 92…96 GHz band S11 is always under 11 dB (fig. 3). The computed total efficiency is 0.7908 @ 92 GHz, 0.7640 @ 94 GHz and 0.7418 @ 96 GHz. Directivity is 22.01 dBi @ 92 GHz, 22.37 dBi @ 94 GHz and 22.30 dBi @ 96 GHz.

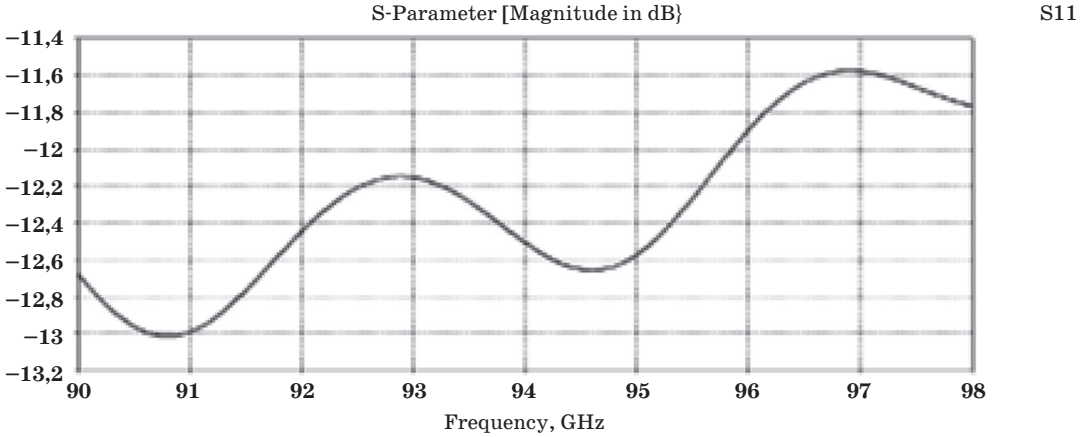

Fig. 3. S11 for horn antenna

Far-field radiation patterns are shown for 92, 94 and 96 GHz in XZ and YZ planes (fig. 4).

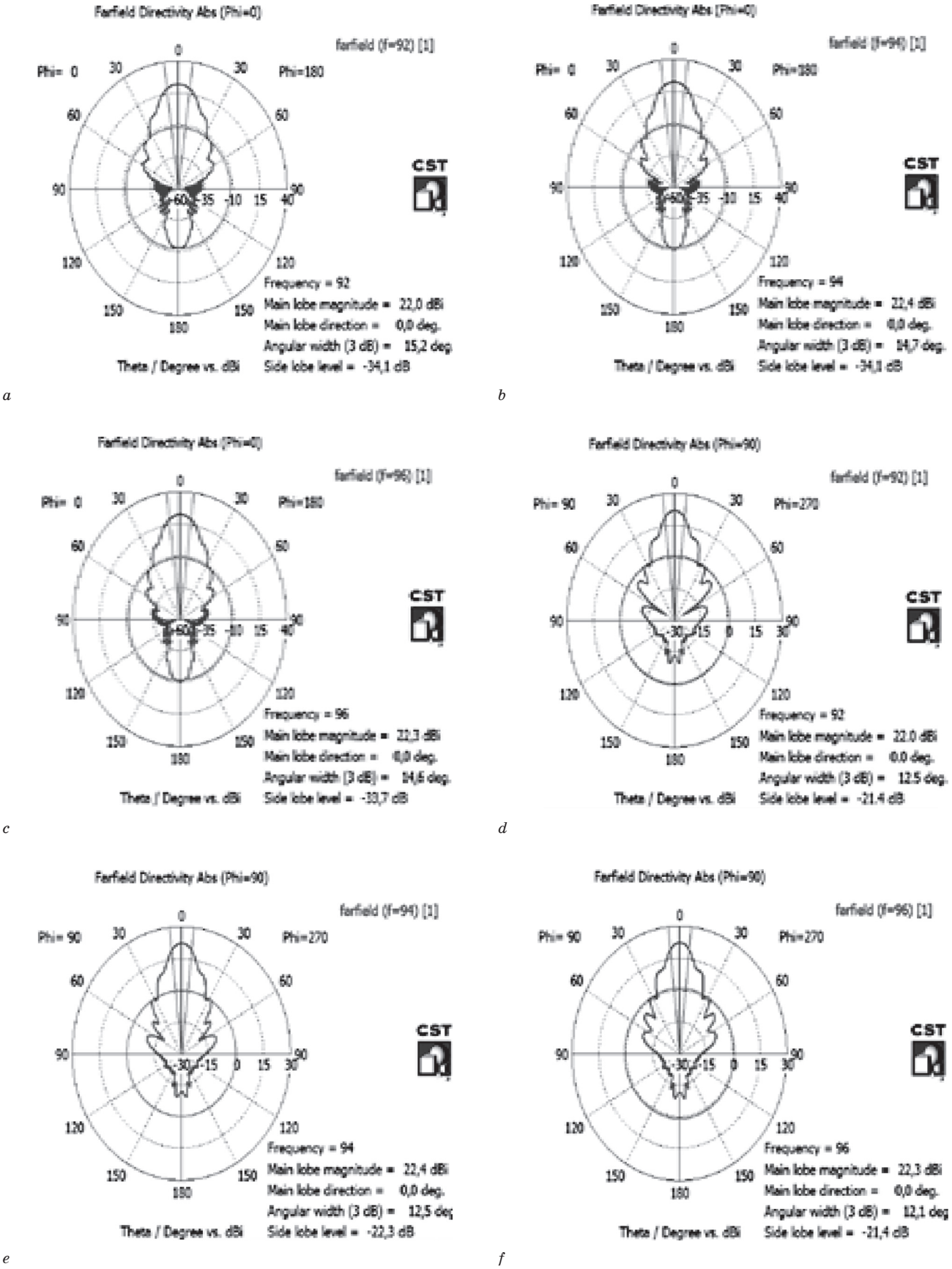

Fig. 4. Far-field patterns: *a* — 92 Hz, XZ plane; *b* — 94 Hz, XZ plane; *c* — 96 Hz, XZ plane; *d* — 92 GHz, YZ plane; *e* — 94 GHz, YZ plane; *f* — 96 GHz, YZ plane

Near-field result

A post processing tool has been used to obtain near-field patterns at various distance from horn mouth at 94 GHz (fig. 5). Angular width and spot radius (3 dB) are summarized in table 2. A comparison of the patterns is shown in fig. 5, *a* and 5, *b*.

Origin of the post-processing tool for near-field patterns is inside horn, 1.75 cm far from horn mouth. So it is necessary to add this length to distances showed in table 2 for the calculation of the spot size.

Table 2

Angular width and spot radius (3 dB)

	XZ plane ($N = 0°$)		YZ plane ($N = 90°$)	
Distance, cm	**Angular width, degrees**	**Spot radius, cm**	**Angular width, degrees**	**Spot radius, cm**
1.25	20.8	0.55	24.9	0.66
2.25	11.2	0.39	19.8	0.69
3.25	10.9	0.48	12.9	0.57
4.25	11.3	0.59	11.5	0.60
5.25	11.7	0.72	11.3	0.69
6.25	12.0	0.84	11.2	0.78
7.25	12.3	0.97	11.3	0.89
8.25	12.5	1.10	11.3	0.99
13.25	13.2	1.74	11.6	1.52
18.25	13.5	2.36	11.8	2.07
28.25	13.9	3.65	12.0	3.155

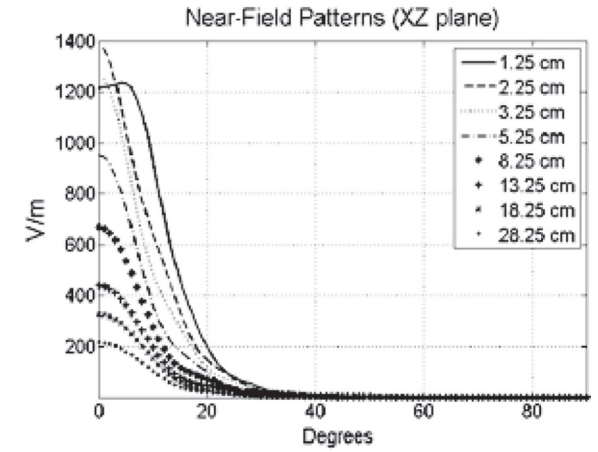

a

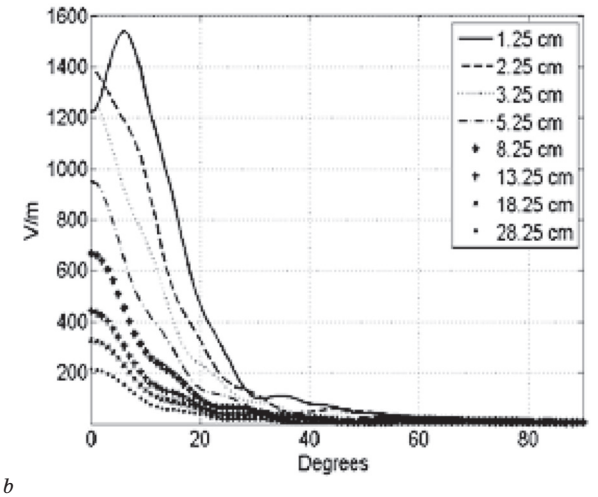

b

Fig. 5. Near-field pattern: *a* — XZ plane; *b* — YZ plane

Near-field result with absorber

Horn Antenna has been simulated inside a microwave absorber (fig. 6). Geometric dimensions of the absorber have been measured and an appropriate CAD model has been designed with these measures. In particular radius of the hole in front of horn mouth is 8 mm and the whole absorber is 12 cm high (from one tip to base). Electromagnetic parameters, instead, have been estimated with an analytical model (dispersion fit 2nd order) due to the impossibility of the manufactures of the microwave absorber to provide us electromagnetic measures at ~100 GHz. Some values of real part of complex electrical permittivity R' and conductibility T necessary for analytical model have been taken from literature [4].

Angular width and spot radius (3 dB) are summarized in table 3. A comparison of the patterns is shown in fig. 7, *a* and 7, *b*. Distance refers to the horn mouth. Minimum distance achievable through post processing tool is 13.25 cm far from horn mouth.

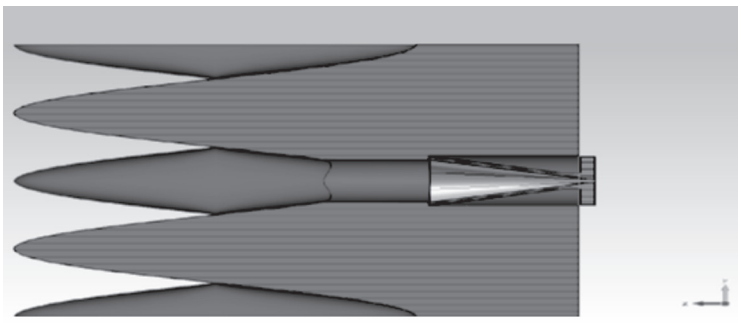

Fig. 6. Lateral view of horn antenna inside absorber

Table 3

Angular width and spot radius (3 dB) with absorber

	XZ plane ($N = 0°$)		YZ plane ($N = 90°$)	
Distance, cm	**Angular width, degrees**	**Spot radius, cm**	**Angular width, degrees**	**Spot radius, cm**
13.25	9.8	1.28	9.0	1.18
16	10.0	1.55	9.4	1.46
20	10.2	1.94	9.8	1.86
25		2.41	10.2	2.39
30	10.4	2.88	10.5	2.92

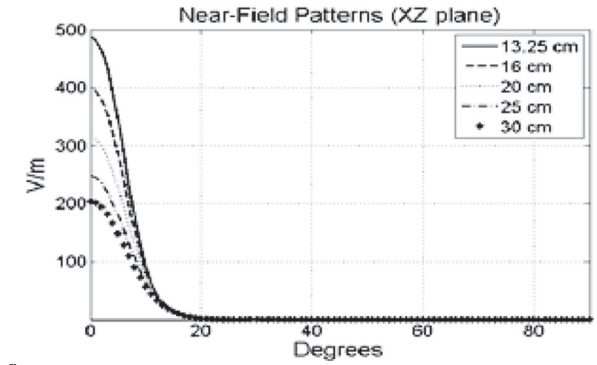

a

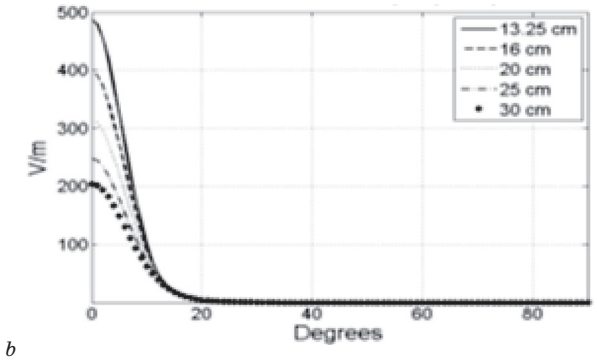

b

Fig. 7. Near-field patterns: *a* — XZ plane, 94 GHz with absorber; *b* — YZ plane, 94 GHz with absorber

Near-field patterns with and without absorber

Fig. 8 shows a comparison between near-field patterns with and without absorber for each distances of our interest in both planes XZ and YZ.

Spot size without absorber and percentage reductions obtained through absorber are summarized in table 4.

Table 4

Spot size without absorber and percentage reduction

	XZ plane ($N = 0°$)		YZ plane ($N = 90°$)	
Distance, cm	**Angular width, degrees**	**Spot radius, cm**	**Angular width, degrees**	**Spot radius, cm**
13.25	1.74	26.1	1.52	21.8
16.2	08	25.5	1.82	19.7
20	2.59	25.1	2.25	17.0
25	3.23	25.4	2.79	14.3
30	3.89	26.0	3.34	12.5

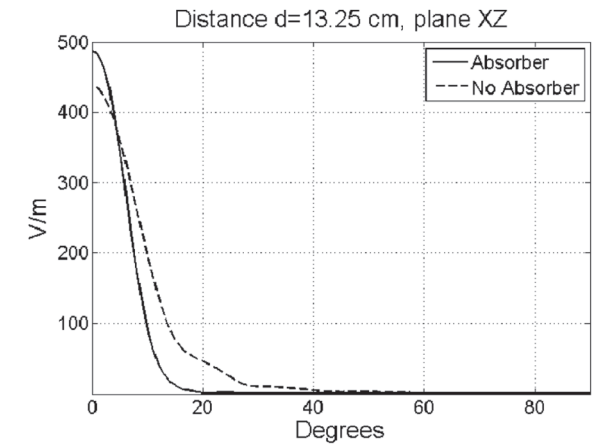

a

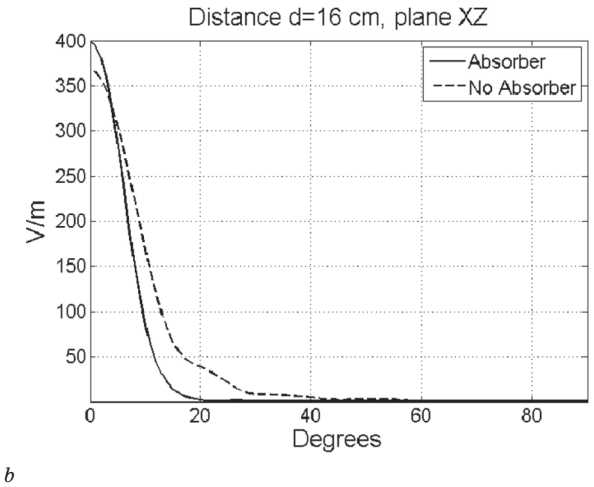

b

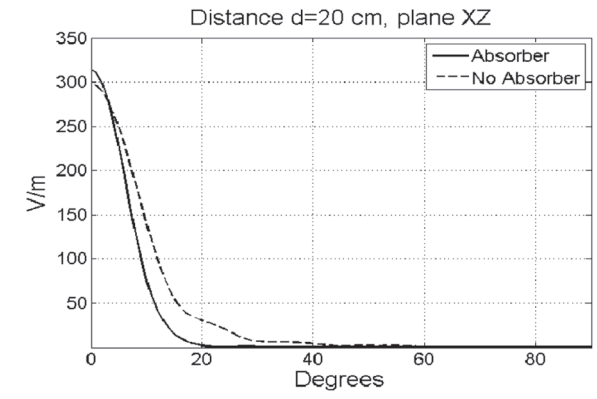

c

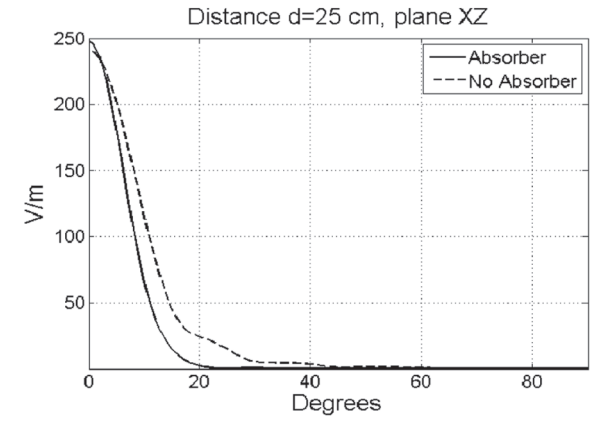

d

Fig. 8. Near-field patterns with and without absorber for various distances *d* in plane XZ and YZ: *a* — *d* = 35.25 cm, plane XZ; *b* — *d* = 16 cm, plane XZ; *c* — *d* = 20 cm, plane XZ; *d* — *d* = 25 cm, plane XZ; *e* — *d* = 30 cm, plane XZ; *f* — *d* = 13.25 cm, plane YZ; *g* — *d* = 16 cm, plane YZ; *h* — *d* = 20 cm, plane YZ; *k* — *d* = 25 cm, plane YZ; *l* — *d* = 30 cm, plane YZ

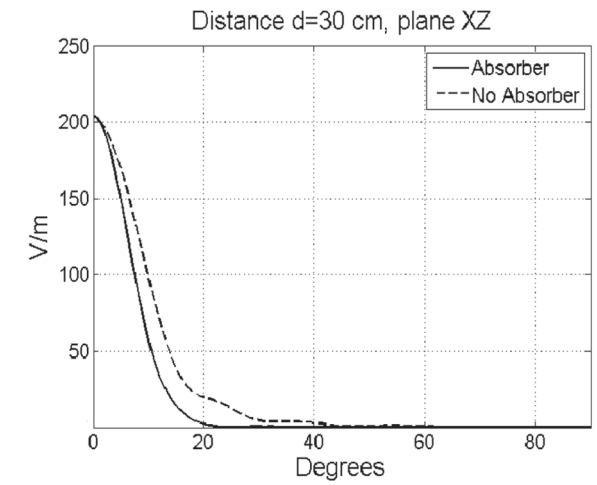

e

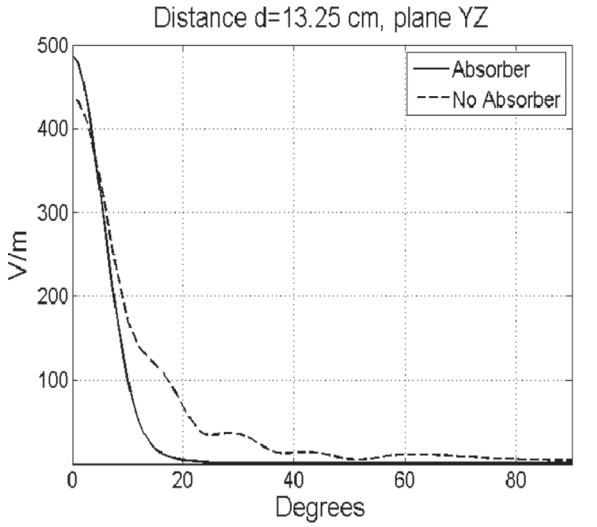

f

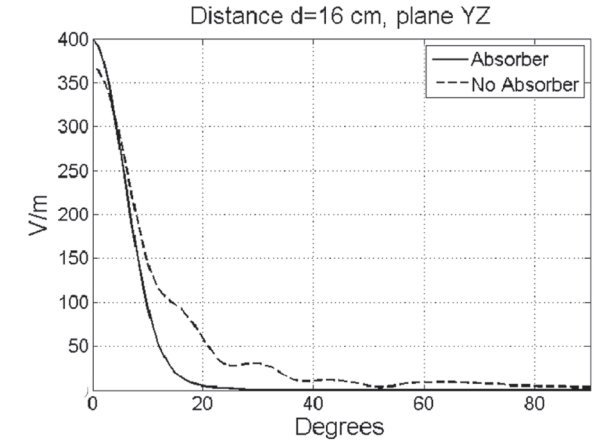

g

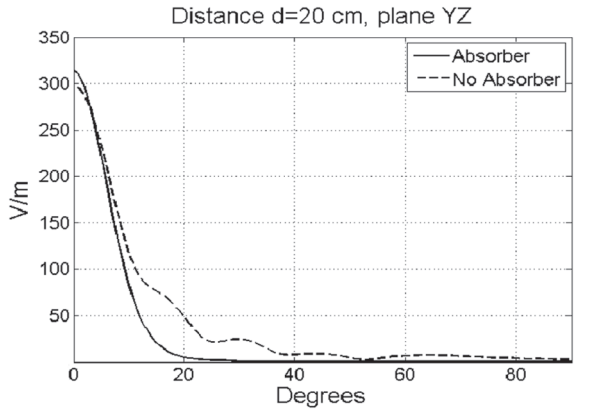

h

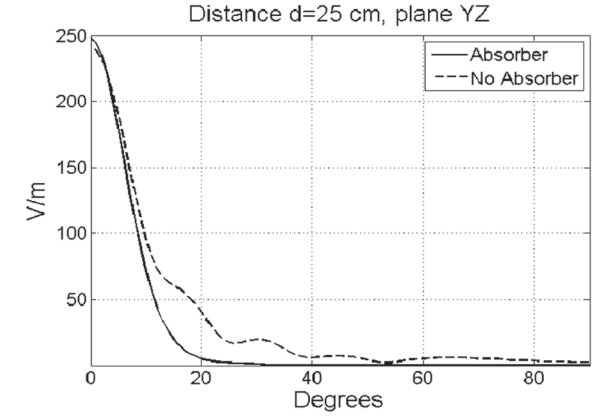

k

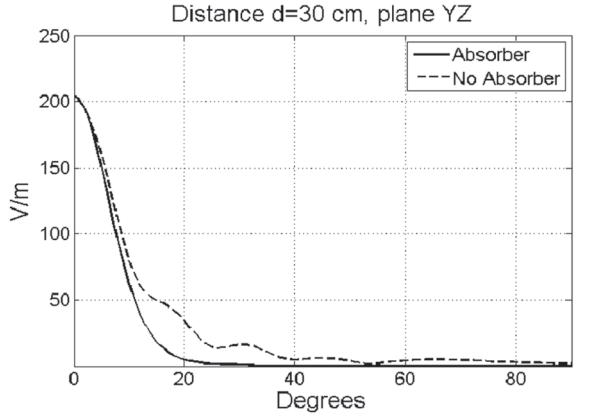

l

Fig. 8. End

CONCLUSIONS

We have simulated antenna in the far field region. Directivity is 22 dBi almost constant in the 92…96 GHz band, total efficiency is between 79% and 74%, and S11 is always under 11 dB. Near field patterns show us that the optimal distance which minimizes spot radius is approximately between 2.25 and 3.25 cm far from horn mouth. At this distance we can obtain an elliptical spot size with major semi-axis (0.63±0.06) cm long and minor semi-axis (0.44±0.05) cm long. A relative minimum is present in the near field patterns, in both planes, at $x = 0°$ when field is simulated with a 1.25 cm distance from horn mouth, then a really carefully position of antenna is necessary.

Using a microwave absorber appropriately placed (see figure 12) is possible to obtain reduction of the spot size. An approximately constant reduction of 25% is achievable in XZ plane. In YZ plane maximum reduction is 21.8 % at a distance of 13.25 cm far from horn mouth. With greater distance, reduction of the spot size achievable is lesser.

REFERENCES

*1. **Vandenbosch, Guy A. E.** Microstrip Antennas / Guy A. E. Vandenbosch and Alexander Vasylchenko: edited by Nasimuddin.— Chapter 21: A Practical Guide to 3D Electromagnetic Software Tools .*

*2. **Website:** http://en.wikipedia.org/wiki/Finite-difference_time-domain_method.*

*3. **Website:** http://www.microwaves101.com/encyclopedia/waveguidedimensions.cfm*

*4. **Косовець, М.** Оцінювання параметрів характеристичних функцій 3D терагерцового радара / М. Косовець, О. Павлов, В. Смірнов: зб. тез VI Міжнар. наук.-техн. симпозіуму «Нові технології в телекомунікаціях», ДУІКТ–Карпати'2013.— Вишків, 21–25 січня 2013.— С. 174–179.*

*5. **Knap, W.** Signal processing 3D Terahertz Ima-ging FMCW Radar for the NDT of material / W. Knap, N. Kosovets, A. Drobik: сб. тезисов VI Междунар. науч.-техн. симпозиума «Новые технологии в телекоммуникациях», ГУИКТ–Карпаты'2013.— Вышков, 21–25 января 2013.— С. 154–156.*

Рецензент: канд. техн. наук, професор **О. В. Дробик**, Державний університет телекомунікацій, Київ.

М. А. Косовець, Л. М. Товстенко

МОДЕЛЮВАННЯ КОНІЧНОЇ РУПОРНОЇ АНТЕНИ ДЛЯ 3D ТЕРАГЕРЦОВОГО FMCW РАДАРА

Вивчено можливості формування апертури конічної антени. Виміряно близьке і далеке поля антени. Досліджено вплив поглинача на розмір діаграми спрямованості в головному напрямі поширення.

Ключові слова: цифровий спектральний аналіз; рупор антени; електромагнітні симулятори; рівняння Максвелла; метод моментів; метод скінченних елементів.

Н. А. Косовец, Л. М. Товстенко

МОДЕЛИРОВАНИЕ КОНИЧЕСКОЙ РУПОРНОЙ АНТЕННЫ ДЛЯ 3D ТЕРАГЕРЦОВОГО FMCW РАДАРА

Изучены возможности формирования апертуры конической антенны. Измерены ближнее и дальнее поля антенны. Исследовано влияние поглотителя на размеры диаграммы направленности в главном направлении распространения.

Ключевые слова: цифровой спектральный анализ; рупор антенны; электромагнитные симуляторы; уравнение Максвелла; метод моментов; метод конечных элементов.

УДК 621.311.6

В. Б. ТОЛУБКО, доктор техн. наук, професор;
П. В. АФАНАСЬЄВ;
В. М. БОНДАРЕНКО;
М. П. ТРЕМБОВЕЦЬКИЙ, канд. техн. наук, доцент,
Державний університет телекомунікацій, Київ;
Т. В. УВАРОВА,
Державний університет оборони України, Київ

ПОБУДОВА СИСТЕМ ГАРАНТОВАНОГО ЕЛЕКТРОЖИВЛЕННЯ ТЕЛЕКОМУНІКАЦІЙНОЇ АПАРАТУРИ

Розглянуто відомі структури побудови систем гарантованого електроживлення. Проаналізовано переваги і недоліки кожної структури, а також наведено рекомендації щодо використання зазначених систем.

Ключові слова: інвертор; система гарантованого електроживлення; статичний перемикач; By-Pass; електромережа; топологія; випрямляч; акумуляторна батарея.

Вступ

Телекомунікаційна апаратура живиться від промислової електромережі, її надійна робота значною мірою залежить від якості електроенергії. Спотворення по колах живлення тривалістю лише частки мілісекунд можуть впливати на роботу апаратури. Унаслідок цього було виокремлено клас ***систем гарантованого електропостачання (СГЕ)***, які забезпечують належну якість електричної енергії для сучасної апаратури. Такі пристрої мають основне та резервне джерела електричної енергії. Спосіб переходу з основного джерела на резервне та навпаки визначає головні топології побудови СГЕ [1; 3].

Основна частина

Топологія stand-by. У СГЕ, побудованих за цією топологією, у нормальному режимі роботи подача електроенергії на вихід здійснюється безпосередньо з входу електромережі через